Electron density radial profiles derived from Stark broadening in a sodium plasma produced by laser resonance saturation

Mark A. Cappelli and Raymond M. Measures

The first free electron density radial profiles of a sodium plasma created by laser resonance saturation are reported. The measurements were based on Stark broadening of the 4^2D–3^2P multiplet and reveal the formation of a conically shaped plasma along the path of the laser pulse, which can be attributed to strong absorption of the laser pulse along the ionization path.

I. Introduction

Electron density measurements from the Stark broadening of spectral emission lines has developed into a useful and common diagnostic tool since the formulation of reliable Stark broadening theories.[1–4] The most attractive feature of this technique is that it is noninvasive and has been widely used in applications where plasma ionization probes either directly interfere with the processes studied or are easily contaminated by highly reactive constituents of the plasma. The viability of the technique was clearly demonstrated by Agnew and Reichelt[5] in determining the electron density in a cesium plasma diode and afterward in wall stabilized arcs[6–10] where cylindrical symmetry and plasma stability permitted the Abel inversion of lateral intensity measurements to obtain the local emission coefficient and hence the radial variation in electron density. Concurrently, Stark broadening has been widely investigated and employed as a diagnostic tool in transient plasmas produced in shock tubes,[11–14] laser ablation of solid targets,[15,16] low-induction vacuum sparks,[17,18] and plasmas produced by laser resonance saturation.[19–21] Most of these, however, were spatially and/or temporally averaged, depending on the nature or reproducibility of the source. In some cases, multishot averaging has been performed.[20,21] The question of multishot averaging in highly nonlinear systems, such as a plasma column produced by laser resonance pumping, has been addressed in a numerical simulation of the spectral emission of a sodium plasma and is described elsewhere.[22]

In this paper, we report on the measurement of the radial variation of the electron density in a sodium plasma column produced by laser saturation of one of the 3^2S–3^2P resonance transitions. This process has been found to lead to high degrees of ionization in both alkali[19–21,23–25] and alkaline earth[26,27] metal vapors in the 10^{15}–10^{17}-cm^{-3} atom density range. At comparable electron densities, lines of the n^2D–3^2P series in sodium suffer significant electron Stark broadening. We have elected to use Stark broadening of the 4^2D–3^2P transition in sodium to measure the electron density. The broadening of this transition and its equivalent in potassium has been studied extensively,[6,28–30] providing a fair degree of confidence in using the tabulated values for the electron Stark widths and shifts of Griem[4] and Dimitrijević and Sahal-Bréchot.[31] The electron densities are derived from the local emission coefficients, which in turn are obtained from the Abel inversion of the lateral spectral radiances measured perpendicular to the direction of laser propagation into sodium vapor confined within a specially designed heat sandwich oven.[32]

In the case of sodium the visible wavelength spectral lines of interest terminate on either the ground or resonance state. Unfortunately, spectral lines terminating on the ground state will always suffer severe radiation trapping and are of minimal use for spectroscopic measurements. Furthermore, in conditions of laser resonance saturation the lines terminating on either of the 3^2P levels can be influenced by the intense radiation field of the laser and suffer radiation trapping due to the large population of atoms excited into the resonance state by the laser field. This appears to preclude measurements of the free electron density N_e during the period of laser radiation. However, this

The authors are with University of Toronto, Institute for Aerospace Studies, 4925 Dufferin Street, Downsview, Ontario M3H 5T6.

Received 4 September 1986.
0003-6935/87/061058-10$02.00/0.

limitation might be avoided if IR spectral lines terminating on the 4^2S level are employed.

Lines that terminate on the $3p$ levels can provide meaningful data after the laser field has sufficiently diminished and the excess $3p$-resonance state population has had adequate time to decay by means of spontaneous emission and electron collision quenching. Since the electron density and the temperature will vary considerably across the plasma column created by the laser pulse, it is necessary to undertake an elaborate series of measurements across the plasma column, then perform an appropriate inversion to ascertain the radial variation of N_e. This inversion was made much simpler by our assumption of azimuthal symmetry.

A. Theory of the Measurement

The spectral radiance at wavelength λ, arising from the nm transition and observed in the x direction at some height y above the axis of a cylindrical plasma column of radius r_0, see Fig. 1, can be expressed in the form

$$J_{nm}(\lambda,y) = \int_{-\sqrt{(r_0^2-y^2)}}^{\sqrt{(r_0^2-y^2)}} \epsilon_{nm}(\lambda,x,y) \times \exp\left[-\int_x^{\sqrt{(r_0^2-y^2)}} \frac{\epsilon_{nm}(\lambda,x^*,y)dx^*}{P(\lambda,x^*,y)}\right]dx, \quad (1)$$

where

$$\epsilon_{nm}(\lambda,x,y) \equiv \frac{hc}{4\pi\lambda} N_n(x,y) A_{nm} L_{nm}(\lambda,x,y) \quad (2)$$

represents the volume emission coefficient with $N_n(x,y)$, the upper state population density at (x,y), A_{nm} is the Einstein spontaneous emission probability, and $L_{nm}(\lambda,x,y)$ is the associated line profile function at (x,y), the shape of which is determined by the many line broadening mechanisms. If the plasma is assumed to be in local thermodynamic equilibrium, we may write

$$P_{mn}(\lambda,x,y) = \frac{2hc^2}{\lambda^5}\{\exp[hc/\lambda k T_e(x,y)] - 1\}^{-1}, \quad (3)$$

which is the blackbody spectral radiance (or Planck function), and $T_e(x,y)$ is the free electron temperature at (x,y).

If the plasma can be regarded as optically thin at this frequency and azimuthally symmetric, we can write

$$J_{nm}(\lambda,y) = 2\int_0^{r_0} \frac{\epsilon_{nm}(\lambda,r)rdr}{\sqrt{(r^2-y^2)}} \quad (4)$$

by introducing $r^2 = x^2 + y^2$. If the plasma emission is imaged onto the entrance slit of a monochromator with the slit aligned in the direction parallel to the cylinder's axis, we can express the output current signal (watts) of a photomultiplier tube positioned at the exit slit in the form

$$I_{nm}(\lambda,y) = S_{nm}\int_{y-\Delta y/2}^{y+\Delta y/2}\int_{z-\Delta z/2}^{z+\Delta z/2} \times \int_{-\infty}^{\infty} J_{nm}(\lambda',y)T(\lambda'-\lambda)d\lambda'dzdy, \quad (5)$$

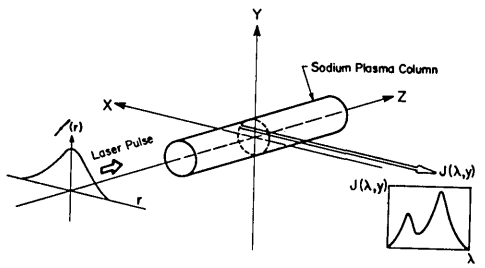

Fig. 1. Geometrical configuration for spectral measurements of sodium plasma created by laser resonance saturation.

where, for long focal lengths and 1:1 imaging, Δy represents the entrance slit width and Δz the slit height. S_{nm} is the photomultiplier sensitivity (A/W) in the vicinity of the wavelength of the nm transition (a slowly varying function of λ over the range of the line spectra), and $T(\lambda' - \lambda)$ is the transmission function of the monochromator and input optics, generally described by a Gaussian function

$$T(\lambda'-\lambda) = \frac{K}{\gamma}\left\{\frac{\ln 2}{\pi}\right\}^{1/2}\exp\left[-\left(\frac{\lambda'-\lambda}{\gamma}\right)^2 \ln 2\right], \quad (6)$$

with γ the instrument halfwidth at half-maximum (HWHM) and K, the filter function, defined by the relation

$$K \equiv \int_{-\infty}^{\infty} T(\lambda'-\lambda)d\lambda, \quad (7)$$

since $T(\lambda' - \lambda)$ is independent of r. Then Eq. (5) can be expressed as

$$I_{nm}(\lambda,y) = S_{nm}\int_y\int_z\left[2\int_0^{r_0}\frac{\epsilon_{nm}(\lambda,r)^*T(\lambda)rdr}{\sqrt{(r^2-y^2)}}\right]dzdy, \quad (8)$$

where * denotes the convolution operation, i.e.,

$$\epsilon_{nm}(\lambda,r)^*T(\lambda) = \int_{-\infty}^{\infty}\epsilon_{nm}(\lambda',r)T(\lambda'-\lambda)d\lambda. \quad (9)$$

The Abel transformation can then be used to provide the corresponding radial distribution of the volume emission coefficient convoluted with $T(\lambda)$:

$$\xi(\lambda,r) = \epsilon_{nm}(\lambda,r)^*T(\lambda) = \frac{-1}{S_{nm}\Delta y\Delta z}\left(\frac{1}{\pi}\right)\int_r^{r_0}\left[\frac{dI_{nm}(\lambda,y)}{dy}\right]\frac{dy}{\sqrt{(y^2-r^2)}}. \quad (10)$$

Equation (2) implies that $\epsilon_{nm}(\lambda,r)$ is directly proportional to the atomic line profile function $L_{nm}(\lambda,r)$. For our experimental conditions, Doppler, resonance, and van der Waals broadening of the 4^2D–3^2P multiplet transition were negligible compared with electron Stark broadening.[33] The contribution to the broadening of the lines by the quasistatic field of the ions is evident as an enhanced red shift which can lead in our conditions, at most, to a 25% increase in the linewidth. Significant red wing asymmetry has not been observed suggesting that Stark broadening due to ions may have a minor effect on the shape of the 4^2D–3^2P emission line. If we ignore the effects of the ions, the Stark profile is Lorentzian in shape with a halfwidth at half-maximum of w and a shift of d, both linearly dependent

on the free electron density N_e. $N_e(r)$ can be evaluated by suitably fitting a Lorentzian function convoluted with a Gaussian [to represent the instrument function in accordance with Eq. (10)] to the Abel inverted radial emission $\xi(\lambda,r)$.

Semiclassical calculations of w and d for isolated neutral lines of sodium have been performed by Griem[1,4] and independently by Dimitrijević and Sahal-Bréchot.[31]

The results for the 4^2D–3^2P multiplet transitions over a wide range of electron temperatures T_e are given in Table I.

A spectral line is considered isolated if the linewidth ($2w$) is much narrower than the separation between either the upper or lower level (having orbital momentum quantum number l) involved in the transition and its nearest interacting level[4] with orbital angular momentum quantum number $l \pm 1$. This describes a critical electron density[31] N_e^*, above which w and d listed in Table I cannot be used. For the 4^2D–3^2P transition in sodium, $N_e^* \simeq 6 \times 10^{16}$ cm^{-3}.

The Abel inversion is performed using the procedure proposed by Deutsch.[34] The lateral distribution of the line of sight spectral radiance from a plasma of nondimensionalized radius, can be approximated by the product of a polynomial and an exponential function, namely,

$$I_{nm}(\lambda,Y) = \left\{\sum_{k=0}^{N} a_k Y^{2k}\right\} \exp(-\alpha Y^2), \tag{11}$$

where we define the nondimensionalized variables $Y = y/r_0$ and $R = r/r_0$. In these conditions direct integration enables us to write

$$\xi_{nm}(\lambda,R) = -\frac{1}{\pi}\sum_{k=0}^{N} b_k f_k(R), \tag{12}$$

where

$$b_k = \begin{cases} 2(k+1)a_{k+1} - 2\alpha a_k, & \text{for } 0 \le k \le N-1, \quad (13) \\ -2\alpha a_k, & \text{for } k = N, \quad (14) \end{cases}$$

and

$$f_k(R) = \sum_{p=0}^{K} \frac{k!}{(k-p)!p!} R^{2p}\Big\{(2\alpha)^{p-k-1}(\alpha\pi)^{1/2} \times \exp(-\alpha R^2)\,\mathrm{erf}[\alpha(1-R^2)]^{1/2} - \exp(-\alpha)\sum_{s=1}^{k-p}(2\alpha)^s(1-R^2)^{k-p-s+\frac{1}{2}}\Big\}, \tag{15}$$

where the last sum vanishes for $p = k$, and erf denotes the error function. Although Eq. (15) is fairly complicated, it is not too difficult to evaluate numerically since in most practical situations four or five terms are adequate.[33] Indeed, in our analysis we have found that we can represent the lateral emission profiles by a function of the form[33]

$$I(y) = \{a_0 + a_1 y^2 + a_2 y^4\} \exp(-\alpha y^2), \tag{16}$$

where the fitting parameters a_0, a_1, a_2, and α are chosen to minimize the residual sum of the squares of the deviations from the actual data.

Table I. Comparison of Theoretical Electron Impact Stark Halfwidths and Shifts at $N_e = 1.0 \times 10^{16}$ cm^{-3}

	d (Å)		w (Å)	
T_e (K)	Griem[4]	D-SB[31]	Griem[4]	D-SB[31]
2500		0.809		1.125
5000	0.920	0.773	1.44	1.105
10000	0.805	0.672	1.35	1.055
20000	0.647	0.552	1.23	0.985

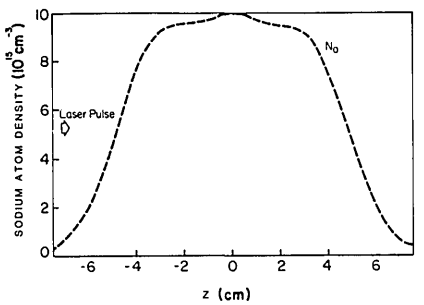

Fig. 2. Experimentally determined neutral sodium density variation along the direction of laser propagation.

II. Experimental Facility and Results

At the heart of our laser ionization based on resonance saturation (LIBORS) facility is a Nd:YAG (JK-HY750) laser, the second harmonic of which pumps a dye laser (Quanta-Ray PDL-1). The sodium vapor is confined to a disklike distribution within a specially designed heat sandwich oven that provides 360° optical access. A detailed description of this novel oven and the method of measuring the sodium atom density distribution is provided elsewhere.[32] The neutral sodium atom density distribution along the direction of laser propagation, measured for the particular experiment described here, is shown in Fig. 2.

The electron density measurements were undertaken using a sideways mounted SPEX 1700 II monochromator. This enables the entrance slit of the monochromator to sample a thin horizontal slab of the plasma emission at a height y (scanned by adjusting the input optics) above the axis of the laser beam. The magnification of the optics was 1:1 with the SPEX entrance slit at 1 cm × 40 μm. A schematic overview of the facility is present as Fig. 3.

The signal from the RCA C31034 photomultiplier mounted on the SPEX monochromator was processed by an EG&G 4420 signal averager that was typically gated to sample the emission in a 2-ns interval, some 65 ns after the start of the laser pulse. Since the laser pulse duration was <40 ns (a near Gaussian temporal profile with FWHM = 14 ns), the influence of the laser field (through the dynamic Stark effect) should be minimal and spontaneous, and electron collision-induced decay of the resonance state population should minimize optical depth effects.

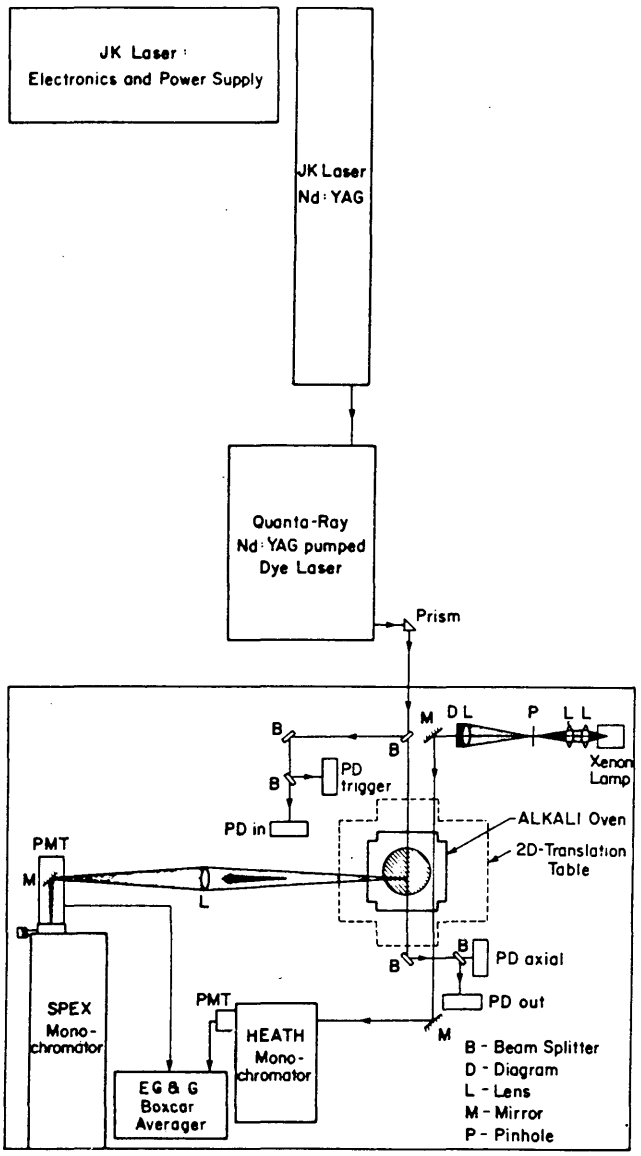

Fig. 3. Schematic overview of LIBORS facility.

To evaluate the radial profile of the free electron density $N_e(r)$, spectral scans of the 4^2D–3^2P multiplet were taken for fifteen positions across the plasma column. The spectral resolution was estimated to be 0.05 nm (FWHW) with sixteen laser shots being averaged to constitute one intensity measurement (at a given wavelength), and 128 such measurements comprise one spectral scan. A set of representative spectral scans of the 4^2D–3^2P multiplet recorded 65 ns after the start of the laser pulse at $z = -2$ cm and $z = 2$ cm (laser pulse enters from $z = -\infty$) are presented as Fig. 4. The emission arising for small lateral displacements are seen to suffer a much greater Stark broadening and red shift than the emission originating from the more weakly ionized rim of the plasma column. The difference in broadening between $z = -2$ cm and $z = 2$ cm indicates that the electron density of the plasma is decreasing along the path of the laser pulse. The laser in this run was tuned to the 589.6-nm resonance line, and the energy incident on the sodium vapor was ~25 mJ. In this experiment, the incident laser beam was collimated (unfocused) with a beam radius of 2.5 mm. The peak sodium atom density occurs at $z = 0$ and was estimated to be $\sim 1.0 \times 10^{16}$ cm^{-3} (see Fig. 2).

Two representative inverted (4^2D–3^3P) multiplet spectra for $z = -2$ cm and $r = 1.2$ mm and $z = 2$ cm and $r = 0.3$ mm are displayed as O data points in Fig. 5. Each inverted multiplet spectrum was then fitted by three theoretically computed Stark electron impact broadened profiles that have been convoluted with a Gaussian function having 0.05-nm FWHM (curves). This permits us to ascertain both the most likely value for the free electron density and the spread in this value for each radial position. For the curves depicted in Fig. 5, we used the Stark widths and shifts of Griem,[4] and the temperature of the free electrons was taken to be 5000 K. The basis of this claim is an independent measurement of T_e from the intensity ratio of the 6^2D–3^2P spectral lines.[33] The profiles are quite insensitive to the changes in electron temperature (see Table I) for the present range of conditions and the assumption that $T_e = 5000$ K in the computed spectra should not affect the conclusions. Use of the Stark widths and shifts calculated by Dimitrijević and Sahal-Bréchot[31] would be just as valid (as the results of the two theories agree within their estimated accuracies) and would systematically increase our measurements by ~20% (see Table I). The reversal evident in the spectra around the unshifted line centers of each line is suspected to arise from truncation in the Abel inversion as opposed to self-absorption due to optical depth effects (see Appendix).

In Figs. 6 and 7, we present four inverted multiplet spectra with the theoretically computed Stark broadened profiles for the most likely free electron density. These figures reaffirm the qualitative interpretation of the raw spectral data presented in Fig. 5, that is, the density and radius of the plasma are decreasing along the path of the laser pulse. This deduction is even more graphically illustrated in Fig. 8 where we have evaluated the free electron density radial profiles at $z = -2$ cm (Δ data) and $z = 2$ cm (O data). Also shown are two empirical curves for $N_e(r)$ that represent these data quite well.

These results indicate that, although the sodium atom density is about the same at these two axial positions ($z = -2$ and 2 cm), the radius and peak density of the free electrons are dramatically different. This can be understood in terms of absorption of the laser pulse as it propagates through the sodium vapor. To illustrate this, Fig. 9 shows the temporal profile of the output laser pulse (as detected by a fast photodiode) for laser wavelengths of 588 and 589 nm. The laser beam has been directed through a 1-mm radius aperture to sample the core near $r = 0$. Clearly, >50% of the energy is absorbed when tuned to resonance compared with the 1.0-nm detuned case. This represents a dramatic drop in the laser energy and suggests that laser absorption can be the cause of the difference

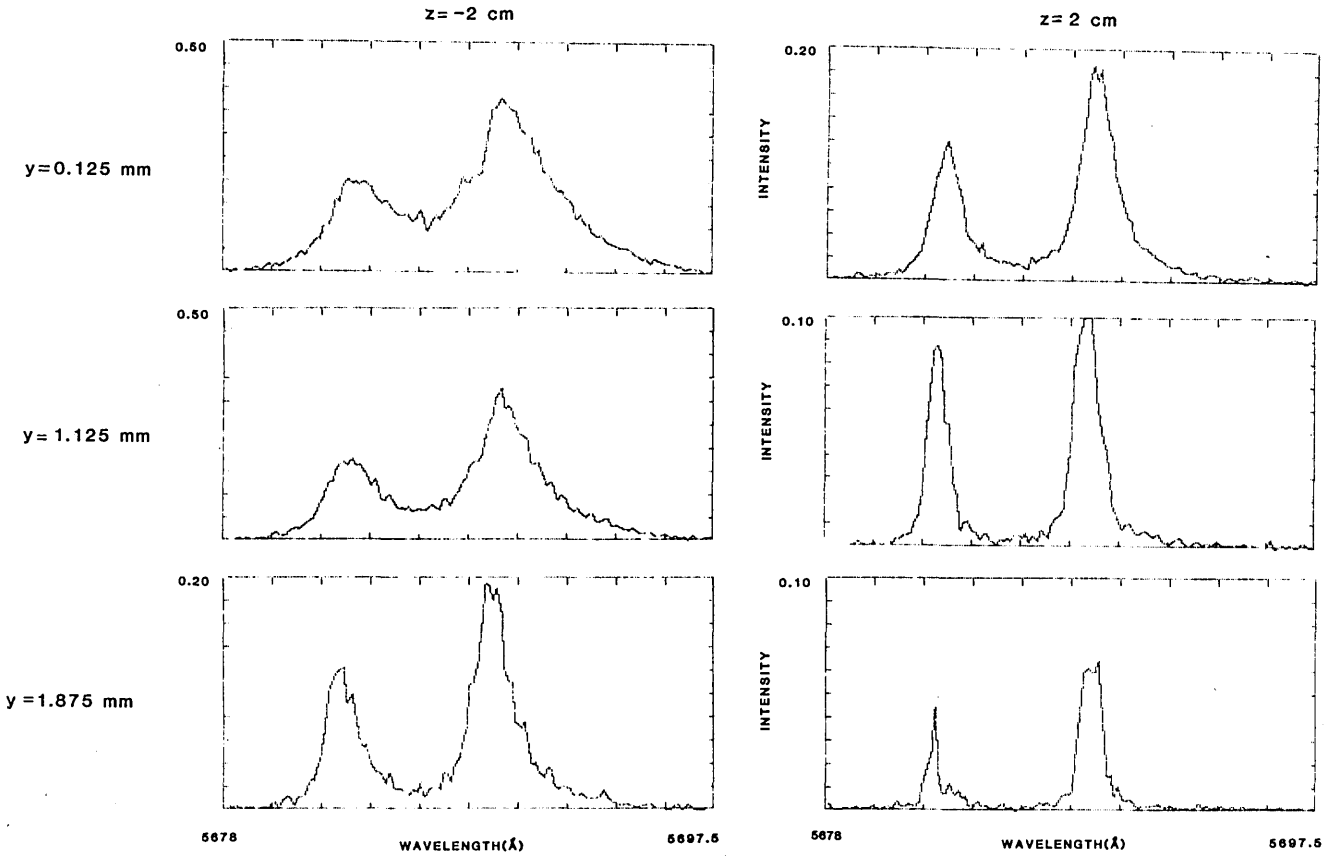

Fig. 4. Set of 4^2D–3^2P sodium multiplet spectra recorded at three y positions and $Z = -2$ and 2 cm.

in the electron density distributions observed at $z = -2$ and 2 cm along the laser path. A comparison between these experimentally evaluated free electron density radial profiles and those predicted on the basis of a computational model of LIBORS, which takes into account this laser absorption, is presented elsewhere.[35]

As a check on the consistency of our measurements we computed the optically thin [Eq. (4)] and optically thick [Eq. (1)] multiplet spectrum that would be observed at $z = -2$ cm and $y = 1.125$ mm corresponding to the free electron density radial profile at $z = -2$ cm (see Fig. 8) and compared these spectra with the measured multiplet spectrum (+) at $z = -2$ cm and $y = 1.125$ mm.

The computed multiplet spectra were obtained by first deriving the radial profile of the free electron temperature at $z = -2$ cm using the Saha equation, the analytical fit to the free electron density radial distribution, and the initial sodium atom density. This temperature distribution, combined with the assumption of LTE, allowed us to ascertain the radial profiles of the 4^2D and 3^2P population densities. The multiplet spectrum observed at any given lateral y position was then determined by solving the radiative transfer equation assuming that either the 3^2P population was zero everywhere (optically thin solution) or as determined above in LTE conditions (optically thick solution.[33]

This comparison is presented as Fig. 10 and suggests that the distortion to the profiles due to optical depth is within experimental uncertainty and can be neglected. Both of the computed spectra are in good agreement with the experimental data, implying that optical depth plays a minor role in interpretation of the Stark broadened spectra.

As a further check on our measurements we compared the computed 4^2D population density radial profiles at $z = -2$ and 2 cm (curves) with the normalized (at $r = 0$) 4^2D population density radial profiles (data points Δ and O) derived by inverting the spectrally integrated experimental lateral emission profiles. This comparison is presented as Fig. 11 and indicates a general, but not exact, agreement.

III. Conclusions

Sodium vapor, confined within a specially designed heat sandwich oven, has been ionized by a pulse of laser radiation tuned to saturate one of the resonance lines. We have undertaken the first experimental evaluation of the plasma's free electron density radial profile at several locations along the path of the laser pulse. These measurements were based on matching the radially inverted (4^2D–3^2P) multiplet spectral data with the convoluted Stark (electron impact) and instrumental broadened profiles. The results clearly reveal that the plasma formed by this interaction is strongly

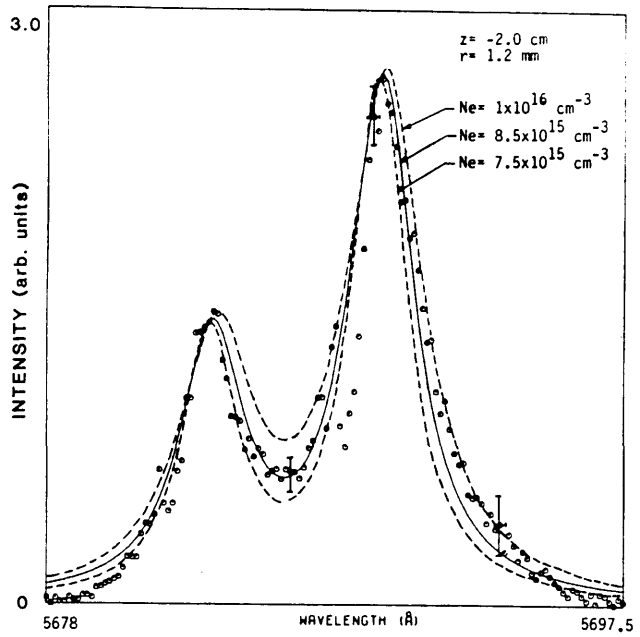

a)

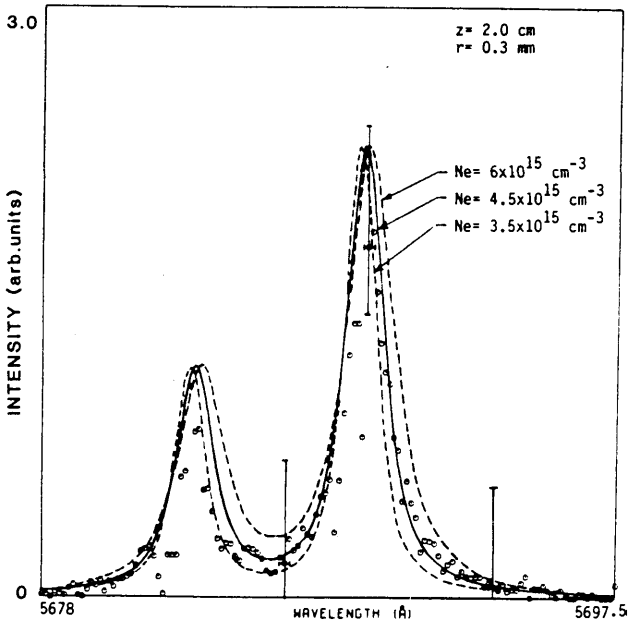

b)

Fig. 5. Fitting of Stark and instrument profiles to the experimental spatially inverted 4^2D–3^2P sodium multiplet spectra at (a) $Z = -2$ cm, $r = 1.2$ mm and (b) $Z = 2$ cm, $r = 0.3$ mm.

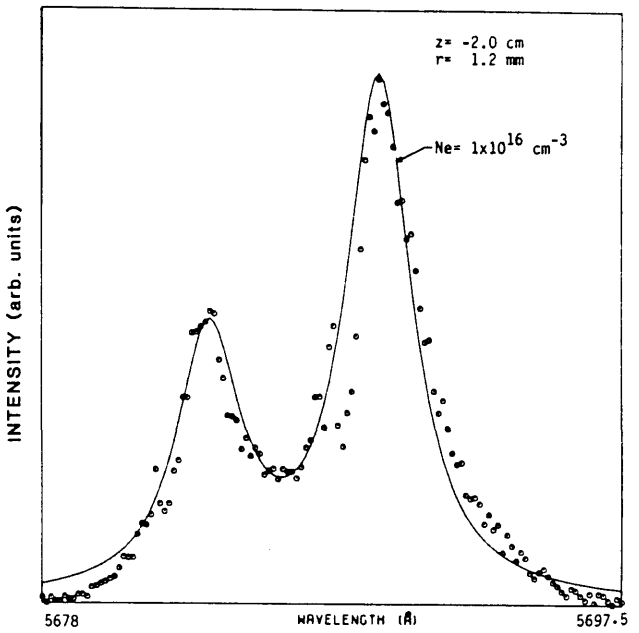

a)

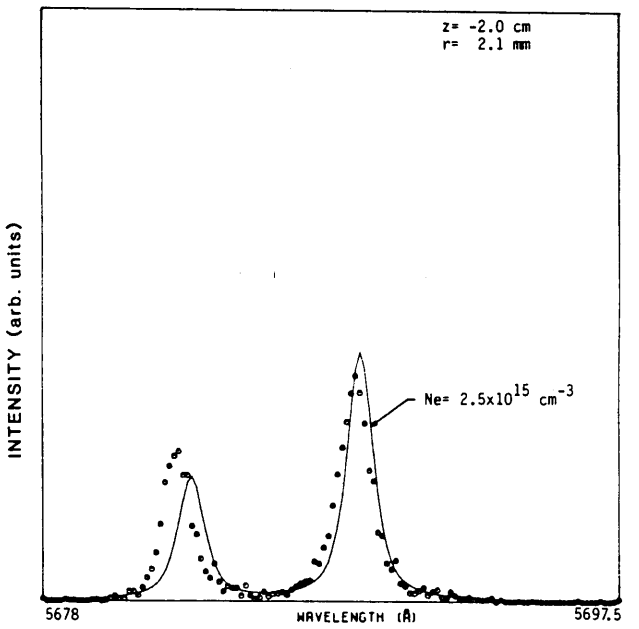

b)

Fig. 6. Best fit of Stark and instrument profiles to the experimental spatially inverted 4^2D–3^2P sodium multiplet spectra at (a) $Z = -2$ cm, $r = 1.2$ mm and (b) $Z = -2$ cm, $r = 2.1$ mm.

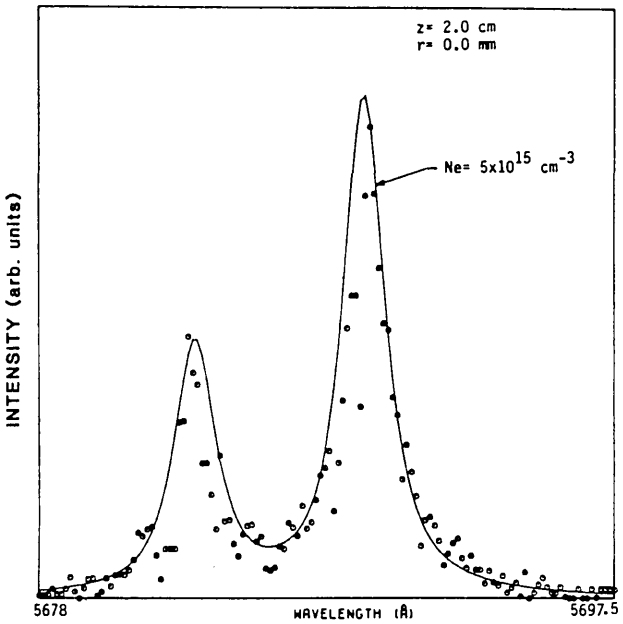

a)

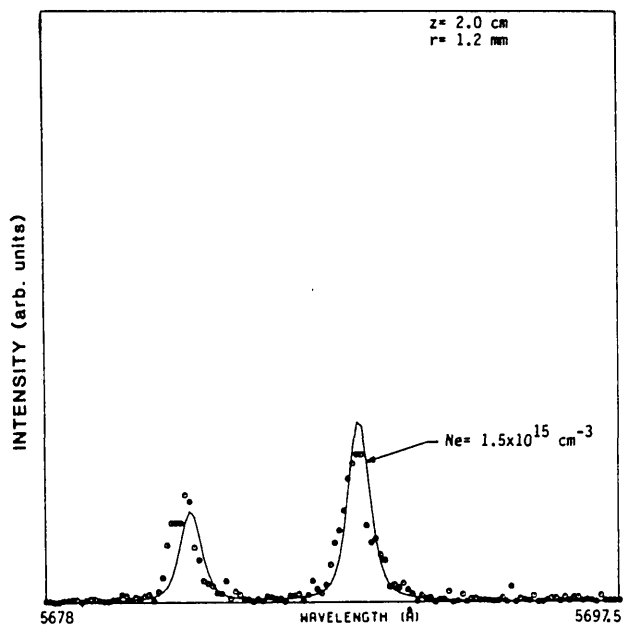

b)

Fig. 7. Best fit of Stark and instrument profiles to the experimental spatially inverted 4^2D–3^2P sodium multiplet spectra at (a) $Z = 2$ cm, $r = 0$ mm and (b) $Z = 2$ cm, $r = 1.2$ mm.

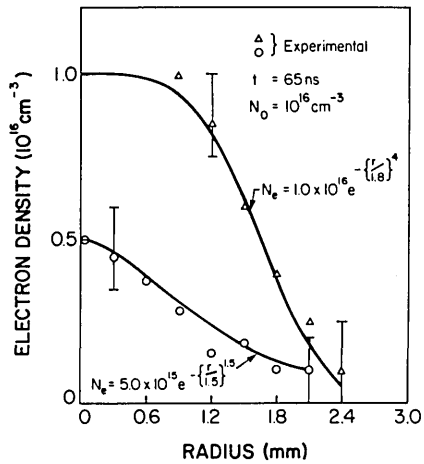

Fig. 8. Experimentally determined electron density radial profiles at $Z = -2$ and 2 cm in a sodium plasma created by laser resonance saturation. Also shown are analytical fits to the experimental data.

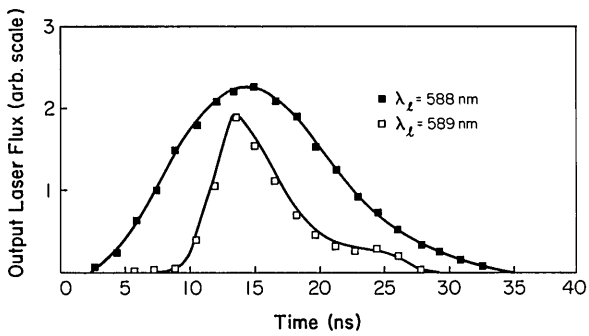

Fig. 9. Photodiode traces of the output laser pulse showing the laser absorption when tuned to 589 nm (○) compared with 588 nm (●).

conical in nature. This could be interpreted in terms of severe absorption of laser energy and is in keeping with the predictions of our computational analysis.[35] This analysis models the interaction both radially and along a finite depth of sodium vapor and has indicated that the free electron temperature can be quite low ($\lesssim$4000 K) after the laser pulse has appreciably penetrated the vapor. These findings could account for the lack of ionization noted by Bowen and Thorpe[36] and the low electron temperature observed by Landen *et al.*[21] as neither set of authors seemed to have appreciated the degree of laser absorption arising in their experiments.

This work was supported by the U.S. Air Force Office of Scientific Research (under grant AFOSR 85-0020) and the Natural Science and Engineering Research Council of Canada.

Appendix: Analytical Example

As indicated in the text premature truncation of the Abel transformation can lead to an apparent self-reversal in the inverted spectra at the line center frequency. We shall use an analytical example to demonstrate the kind of error introduced into the inverted

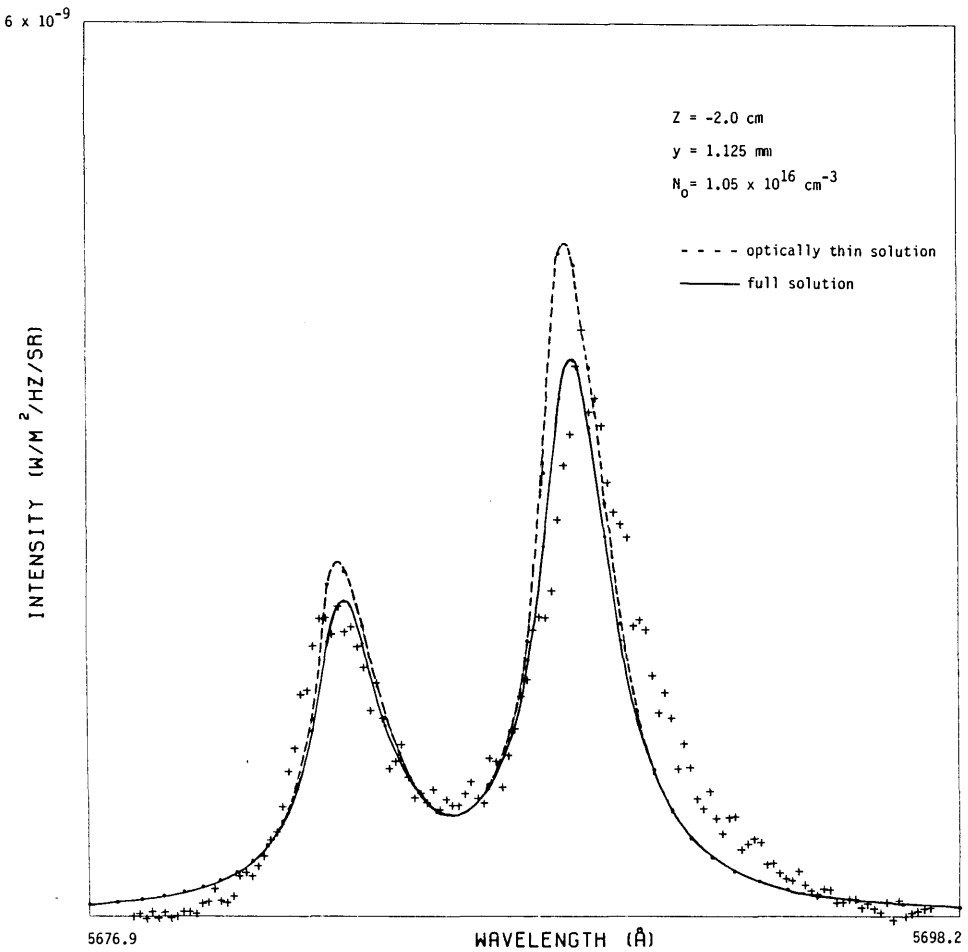

Fig. 10. Comparison of computer generated optically thin and optically thick spectra derived from the measured radial electron density profile (assuming LTE) with the experimental spectrum (data points) at $Z = -2$ cm, $y = 1.125$ mm.

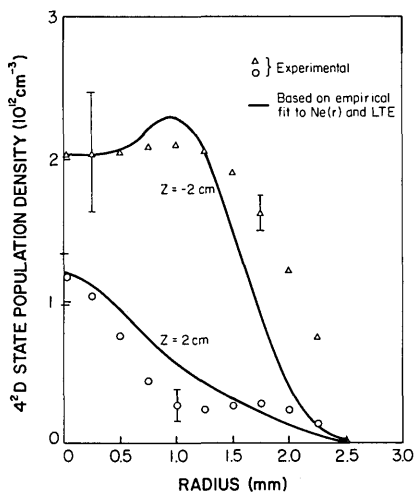

Fig. 11. Comparison of the radial distribution of the 4^2D population of sodium atoms derived from the empirical fit to $N_e(r)$ (assuming LTE) and the radially inverted 4^2D–3^2P emission (normalized at $r = 0$) for $Z = -2$ and 2 cm.

spectrum by truncating the cylindrical plasma's radius.

Equation (10) can be written as

$$\xi(r) = \xi_0 \int_r^{r_0} \frac{\left[\frac{dI(y)}{dy}\right] dy}{\sqrt{(y^2 - r^2)}}, \tag{A1}$$

where we have removed explicit wavelength dependence. If, for example, the lateral emission distributions is Gaussian, we can write

$$I(y) = a_0 \exp(-\alpha y^2), \tag{A2}$$

where

$$\alpha = 1/\gamma^2,$$

and γ is seen to be the $1/e$ radius of the lateral emission distribution. In these circumstances

$$\xi(r) = -2\alpha a_0 \xi_0 \int_r^{r_0} \frac{y \exp(-\alpha y^2) dy}{\sqrt{(y^2 - r^2)}}, \tag{A3}$$

which can be directly integrated to yield

$$\xi(r) = -2a_0\xi_0\sqrt{\alpha} \exp(-\alpha r^2) \operatorname{erf}[\sqrt{\alpha(r_0^2 - r^2)}]. \tag{A4}$$

For large cutoff values so that $r_0/\gamma \gg r/\gamma$ and $r_0/\gamma \gg 1$,

$$\xi(r) = \xi_\infty(r) = \frac{-a_0\xi_0}{\gamma} \exp[-(r/\gamma)^2], \tag{A5}$$

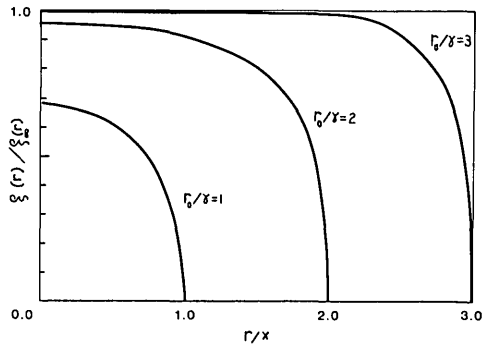

Fig. 12. Variation of the fractional reduction in the inverted emission with reduced radius for truncation equal to one, two, and three Gaussian radii.

and the radially inverted distribution is also seen to be Gaussian.

We can now relate the radial emission profile $\xi(r)$ to that which would be observed in the absence of a cutoff radius, namely,

$$\xi(r)/\xi_\infty(r) = 2\,\mathrm{erf}\left\{\left[\left(\frac{r_0}{\gamma}\right)^2 - \left(\frac{r}{\gamma}\right)^2\right]^{1/2}\right\}. \qquad \text{(A6)}$$

Figure 12 displays the ratio $\xi(r)/\xi_\infty(r)$ for values of $r_0/\gamma = 1, 2$, and 3. For truncation at the $1/e$ value ($r_0/\gamma = 1$), the striking feature is that the inverted emission at $r = 0$ [$\xi(0)$] is 68% of that which one would expect for no truncation. This figure rapidly increases to ~95% for $r_0/\gamma = 2$, which clearly demonstrates the sensitivity of the inversion to truncation and the care that must be taken to avoid serious truncation error over the spectral interval of interest. An apparent self-reversal arises in the inverted spectrum because in reality the plasma emission radius is much greater at the line center wavelengths than in the wings of the spectral lines.

References

1. M. Baranger, in *Atomic and Molecular Processes*, D. R. Bates, Ed. (Academic, New York, 1962).
2. H. R. Griem, *Plasma Spectroscopy* (McGraw-Hill, Toronto, 1964).
3. S. Sahal-Bréchot, "Impact Theory of the Broadening and Shift of Spectral Lines due to Electrons and Ions in a Plasma," Astron. Astrophys. **1**, 91 (1969).
4. H. R. Griem, *Spectral Line Broadening by Plasmas* (Academic, New York, 1974).
5. L. Agnew and W. H. Reichelt, "Identification of the Ionic Species in a Cesium Plasma Diode," J. Appl. Phys. **39**, 3149 (1968).
6. J. Gumberg, G. Coulaud, and Nguyen-Hoe, "Stark Broadening of Sodium Lines Emitted by a Sodium Argon Mixture Plasma," Phys. Lett. A **57**, 227 (1976).
7. V. Helbig, D. E. Kelleher, and W. L. Wiese, "Stark Broadening Study of Neutral Nitrogren Lines," Phys. Rev. A **14**, 1082 (1976).
8. J. H. Waszink and H. J. Flinsenberg, "Determination of the Electron Density in a High Pressure Na-Xe Discharge from the Profile of a Stark-Broadened Spectral Line," J. Appl. Phys. **49**, 3792 (1978).
9. D. E. Kelleher, "Stark Broadening of Visible Neutral Helium Lines in a Plasma," J. Quant. Spectrosc. Radiat. Transfer **25**, 191 (1981).
10. C. Goldbach, G. Nollez, P. Plomdeur, and J. P. Zimmermann, "Stark-Width Measurements of Neutral and Singly Ionized Magnesium Resonance Lines in a Wall Stabilized Arc," Phys. Rev. A **25**, 2596 (1982).
11. M. Neiger and H. R. Griem, "Experimental Investigation of Stark Broadening and Plasma Polarization Shift of Ionized Helium Resonance Lines," Phys. Rev. A **14**, 291 (1976).
12. J. F. Bauer and J. Cooper, "Shock Tube Study of Line Broadening in a Temperature Range of 6100 to 8300K," J. Quant. Spectrosc. Radiat. Transfer **17**, 311 (1977).
13. W. T. Chiang, D. P. Murphy, Y. G. Chen, and H. R. Griem, "Electron Densities from Stark Widths of HeI 5016Å and HeI 3889Å Lines and Helium-Neon Laser Interferometry," Z. Naturforsch. Teil A **32**, 818 (1977).
14. P. H. M. Vaessen, J. M. L. Van Engelen, and J. J. Bleize, "Stark Width Measurements of Argon-Ion Lines with a Fabry-Pérot Interferometer," J. Quant. Spectrosc. Radiat. Transfer **33**, 51 (1985).
15. S. Hashimoto and N. Yamaguchi, "Observations of Stark-Shifts of Lyman-α Lines of Low-Z Ions in Laser Produced Plasmas," Phys. Lett. A **95**, 299 (1983).
16. R. W. Lee, J. D. Kilkenny, R. L. Kauffman, and D. L. Matthews, "Electron Density from Time Resolved Stark Profiles in Ablation Plasmas," J. Quant. Spectrosc. Radiat. Transfer **31**, 83 (1984).
17. R. U. Datla and H. R. Griem, "Stark Profile Measurements on Lyman Series Lines of Al XIII," Phys. Fluids **21**, 505 (1978).
18. R. U. Datla and H. R. Griem, "Electron Density Measurements Using Stark Profiles of Al XIII," Phys. Fluids **22**, 1415 (1979).
19. M. A. Cappelli and R. M. Measures, "Two-Channel Technique for Stark Measurements of Electron Density Within a Laser-Produced Sodium Plasma," Appl. Opt. **23**, 2107 (1984).
20. D. J. Krebs and L. D. Schearer, "Electron Density Measurements in a Laser Induced Sodium Plasma," J. Chem. Phys. **76**, 2925 (1982).
21. O. L. Landen, R. J. Winfield, D. D. Burgess, J. D. Kilkenny, and R. W. Lee, "Production of Dense Cool Plasmas by Resonance Pumping of Sodium Vapor," Phys. Rev. A **32**, 2963 (1985).
22. R. S. Kissack, M. A. Cappelli, and R. M. Measures, "Computer Modelling of the Multishot Average Spectral Emission from a Laser Created Sodium Plasma" (in preparation).
23. T. B. Lucatorto and T. J. McIlrath, "Laser Excitation and Ionization of Dense Atomic Vapors," Phys. Rev. Lett. **37**, 428 (1976); T. J. McIlrath and T. B. Lucatorto, "Laser Excitation and Ionization in a Dense Li Vapor," Phys. Rev. Lett. **38**, 1390 (1977).
24. T. Stacewicz, "Ionization of Sodium Vapor by Intense Laser Light Tuned to 3*s*–3*p* Transition," Opt. Commun. **35**, 239 (1980).
25. F. Roussel, P. Breger, G. Spiess, C. Manus, and S. Geltman, "Evidence of Super-Elastic Effects in Laser-Induced Ionization of Na Vapour," J. Phys. B **13**, L631 (1980).
26. L. Jahreiss and M. C. E. Huber, "Time Resolved Excitation and Ionization of a Laser-Pumped Ba Vapor," Phys. Rev. A **28**, 3382 (1983).
27. C. H. Skinner, "Efficient Ionization of Calcium, Strontium and Barium by Resonant Laser Pumping," J. Phys. B **13**, 55 (1980).
28. P. E. Oettinger and J. Cooper, "Stark Broadening of the NaI 5682–88Å and 4978–82Å Lines," J. Quant. Spectrosc. Radiat. Transfer **9**, 591 (1969).
29. J. P. Hohimer, "Stark Broadening of Potassium ns-4p and nd-4p Lines in a Wall-Stabilized Arc," Phys. Rev. A **30**, 1449 (1984); "Reply to 'Stark Broadening of Potassium Lines,'" **32**, 676 (1985).
30. N. Konjevic, "Stark Broadening of Potassium Lines," Phys. Rev. A **32**, 673 (1985).

31. M. S. Dimitrijević and S. Sahal-Bréchot, "Stark Broadening of Neutral Sodium Lines," J. Quant. Spectrosc. Radiat. Transfer 34, 149 (1985).
32. M. A. Cappelli, P. G. Cardinal, H. Herchen, and R. M. Measures, "Sodium Atom Distribution Within a Heat Sandwich Oven," Rev. Sci. Instrum. 56, 2030 (1985).
33. M. A. Cappelli, "Electron Density Measurements from Stark Broadened Emission in a Sodium Plasma Produced by Laser Resonance Saturation," UTIAS Report 306 (1987).
34. M. Deutsch, "Abel Inversion with a Simple Analytic Representation for Experimental Data," Appl. Phys. Lett. 42, 237 (1983).
35. M. A. Cappelli, S. K. Wong, R. S. Kissack, and R. M. Measures, "Plasma Channel Formation Based on Laser Resonance Saturation" (submitted to Phys. Rev. A).
36. J. L. Bowen and A. P. Thorne, "Time Resolved Fluorescence and Population Measurements in Laser Pumped Barium Vapour," J. Phys. B 18, 35 (1985).

Announcement of the 45th Annual
DEVICE RESEARCH CONFERENCE
UNIVERSITY OF CALIFORNIA AT SANTA BARBARA
JUNE 22-24, 1987

CONFERENCE CHAIRMAN
Jerry Woodall
IBM
P.O. Box 218
Yorktown Heights, NY 10598
(914) 945-1568

TECHNICAL PROGRAM CHAIRMAN
Greg Stillman
Dept. of Elect & Comp Eng
University of Illinois
1406 W. Green St.
Urbana, IL 61801
(217) 333-3097

TECHNICAL PROGRAM COMMITTEE
Dimitri Antoniadis
Jayant Baliga
Bami Bastani
Bob Calawa
Nick Cirillo, Jr.
Robert Cook
Peter Cottrell
Dan Dapkus
Karl Hess
Tom Jackson
Jim Mikkelson
Ray Milano
Kwok Ng
Yuji Okuto
Jim Rosenberg
Krishna Saraswat
Sam Schichijo
Jerold Seitchik

EX OFFICIO PAST CHAIRMAN
Geoff Taylor

LOCAL ARRANGEMENTS CHAIRMAN
Larry Coldren
Dept of Elect & Comp Eng
University of California
Santa Barbara, CA 93106
(805) 961-4486

The 1987 DRC, sponsored by the IEEE Electron Devices Society, will be held at the University of California at Santa Barbara, CA, Monday, June 22 through Wednesday, June 24, 1987. The DRC and the Electronic Materials Conference (EMC) of the AIME will once again coordinate their activities in order to continue stimulating interactions between device and materials people that have occurred for the past several years. The EMC will be held at the same location on June 24-26. It is suggested that device-oriented papers be submitted to the DRC and that materials-oriented papers be submitted to the EMC. Papers dealing with the impact of materials parameters on device performance are encourged at the DRC.

Papers on the following topics are solicited:

- Advanced Silicon Processing
- Bipolar Devices
- Isolation Technology
- Submicron Devices and Structures
- In Situ Processing & Device Applications
- Thin Insulators & Hot Electron Effects
- SOI and 3D Devices
- Power Devices
- Physics of Ultrasmall Devices
- Sensors and Transducers
- Device and Process Models
- Device Characterization & New Techniques
- CMOS Devices and Technology
- Interconnect Technology
- Integrated Optoelectronics
- Microwave Devices
- Novel Infrared Devices
- III-V FET and Bipolar Devices
- Active Guided Wave Devices
- Optical Sources and Detectors
- Multilayered Heterostructures
- III-V Device Processing
- Radiation Effects (Soft Errors)
- Contact Technology
- Quantum Effect Devices

CALL FOR PAPERS: In order to have a paper considered for presentation at the conference, prospective authors must send twenty-two copies of a summary of their paper to:

Gregory E. Stillman
Department of Electrical and Computer Engineering
University of Illinois
1406 W. Green St.
Urbana, IL 61801
(217) 333-3097

The summary must be one page long and should clearly reflect the contents of the paper (see enclosed instructions). The summary should be in a form suitable for publication (e.g. it should include appropriate literature references) but should contain no figures. The summaries of accepted papers will be reproduced verbatim in the conference program and will be published after the conference in the IEEE Transactions on Electron Devices.

TREASURER
Paul Coleman
Dept of Elect & Comp Eng
1406 W. Green St.
University of Illinois
Urbana, IL 61801
(217) 333-2765